Journal Homepage: http://ijcpe.uobaghdad.edu.iq
Iraqi Journal of Chemical and Petroleum Engineering
Vol. 26 No. 4 (December 2025) 27 – 40
EISSN: 2618-0707, PISSN: 1997-4884

Photocatalytic degradation of a cationic dye using Ag_2O@CuO nanoellipsoidal photocatalyst under ultraviolet irradiation

Danyah M. Mohsen [a, *], Sama M. Al-Jubouri [a], Sirhan Al-Batty [b]

a Department of Chemical Engineering, College of Engineering, University of Baghdad, Al-Jadria, Baghdad, Iraq
b Department of Chemical Engineering, Jubail Industrial College, Jubail, Saudi Arabia

Abstract

The photocatalysis oxidation process is a promising technology within the series of advanced oxidation processes, which implements light-induced catalysts to generate strong oxidative species to eliminate organic pollutants from wastewater treatment. The Ag_2O@CuO photocatalyst was successfully prepared by the co-precipitation method. The developed photocatalyst was characterized using X-ray diffraction, Fourier transform infrared spectroscopy, X-ray fluorescence spectrometer, field-emission scanning electron microscopy, Ultraviolet-Visible diffuse reflectance spectra, and photoluminescence spectra. The Ag_2O@CuO efficiency was examined in the photocatalysis degradation of Rhodamine B (RhB) as a cationic dye under the illumination of ultraviolet light. The effect of various parameters, such as the type of light, photocatalyst dose, initial RhB concentration, and pH of the RhB solution, was studied. The results revealed that 90% degradation was achieved within 90 min at a pH of 6.8, 50 mg of a photocatalyst dose, and 10 mg/L of RhB dye under UV irradiation. However, 98% degradation of RhB dye was achieved at a pH of 10 under the same other conditions mentioned above. The kinetic study was performed based on the experimental data of the oxidative photocatalytic degradation of the RhB dye. The zero-order, pseudo-first order, and modified Freundlich kinetic models were applied to accomplish this study. The results showed that the photocatalytic oxidation of RhB dye by the Ag_2O@CuO heterojunction photocatalyst followed a pseudo-first order kinetic model, with an apparent rate constant of 0.0429 min^{-1}. Furthermore, the Langmuir-Hinshelwood model was used to investigate the RhB photocatalytic degradation kinetics of RhB at concentrations of 5-10 mg/L. The determined value of the intrinsic photocatalytic reaction rate constant was 0.7184 mg/L.min for the Ag_2O@CuO heterojunction photocatalyst. Also, the equilibrium adsorption constant was 0.0767 L/mg for the Ag_2O@CuO heterojunction photocatalyst.

Keywords: Bimetallic oxide; Co-precipitation; Copper oxide; Photocatalysis; Rhodamine B dye; Silver oxide.

Received on 24/10/2025, Received in Revised Form on 04/12/2025, Accepted on 05/12/2025, Published on 30/12/2025

https://doi.org/10.31699/IJCPE.2025.4.3

1- Introduction

Industrial wastewater that contaminates the water resources is one of the main environmental challenges of modern life. Effluents from textile, cosmetic, and pharmaceutical industries contain a wide spectrum of hazardous pollutants, including dyes, heavy metals, and pesticides, which can persist in aquatic ecosystems for long periods [1]. Synthetic dyes pose a serious concern due to their high stability, non-biodegradable nature, and potential carcinogenicity [2]. Rhodamine B (RhB) is a pink cationic organic dye that has been linked to neurotoxicity and carcinogenicity in humans as well as pets. In addition, it harms the skin and eyes. The global production of dyes and pigments is nearly 2 million tons annually, and about 15% of this amount is released into water bodies, further aggravating the problem [3]. Accordingly, various treatment methods have been explored, ranging from conventional approaches such as adsorption, coagulation, and membrane separation to advanced technologies like advanced oxidation processes and biosorption [4, 5]

Current research has focused on developing a method of treating discharged water that can achieve complementary decomposition of organic pollutants. These methods involve advanced oxidation processes (AOPs), which consist of the Fenton process, electrochemical oxidation, catalytic wet air oxidation, ozone-based processes, and photo-oxidation processes [6]. The photocatalysis process is one of the AOPs, and it is considered a promising technology among several methods of water treatment because of its high effectiveness, ecological and cost-effectiveness, and recyclability. The photocatalytic reaction initiates when the photocatalyst absorbs a light photon with energy equal to or exceeding its band gap energy, resulting in the generation of electron-hole pairs (e^-/h^+) on the photocatalyst surface. The h^+ is produced in the valence band (VB) during oxidation reactions, whereas the electron moves to the conduction band (CB), where reduction reactions can occur. Numerous factors influence the photocatalyst's performance, like bandgap, e^-/h^+ pair degradation efficiency, and optical absorption [7].

*Corresponding Author: Email: dania.muhsin1707@coeng.uobaghdad.edu.iq

Various semiconductors can be utilized for the photocatalytic degradation of organic pollutants as photocatalysts, some of them generate reactive oxygen species ($\bullet O_2^-$ and $\bullet OH^-$) when exposed to UV or visible light irradiation [8], such as TiO_2 [9], WO_3 [10], ZnO [11], Ag_2O [12], MoS_2 [13], CuO [14], etc. Copper oxide (CuO) is a black colored solid compound, belonging to the monoclinic crystal system, in which the copper atom is coordinated in a square planar configuration [15]. CuO is a P-type semiconductor that is known as an effective photocatalyst due to its narrow band gap (1.2-3.5) eV, non-toxic, high chemical stability, low-cost syntheses, and high surface area. The combination of noble metals with semiconductors is a promising technique to reduce the rate of recombination and enhance photocatalytic efficacy [16-18]. Silver oxide (Ag_2O) is a kind of P-type semiconductor used in various applications, such as electrochemical processes, oxidation catalysis, and sensors. Ag_2O is well known as a powerful photocatalyst that is used to degrade organic pollutants in water. In addition, Ag_2O has a simple cubic structure with a lattice parameter of 0.472 nm. The band gap of Ag_2O is around 1.2 eV. Another advantage of this semiconductor is its low toxicity to water treatment and antimicrobial nature against pathogens [19, 20].

The heterojunction photocatalyst is constituted of oxidative and reductive photocatalysts that exhibit distinct work functions and positions of their Fermi levels. A fundamental requirement for efficient interfacial charge transfer is that the Fermi level and conduction band of the reductive photocatalyst must be higher than those of the oxidative one. Upon the tangency of the two semiconductors, electrons migrate from the reductive photocatalyst towards the oxidative photocatalyst. The Fermi levels of the oxidative and reductive photocatalysts twist upward and downward, respectively, until a state of equilibrium is achieved between the two levels. At the contact point between the two semiconductors, the holes present in the reductive photocatalyst and the electrons in the oxidative photocatalyst undergo recombination and dissipate due to the influence of electrostatic forces. Conversely, the positively charged holes of the oxidative photocatalyst and the electrons from the reductive photocatalyst, possessing considerable redox potential, thus participate during the photocatalytic reaction [21].

Sibhatu et al. [22] reported that, despite numerous photocatalysis applications of CuO, it has several drawbacks that hinder its efficiency in the photocatalytic degradation of organic pollutants, including the rapid recombination of electrons and holes, which reduces the population of radicals responsible for pollutants decomposition. Furthermore, CuO exhibited poor chemical stability under radiation conditions and tends to form accumulations that reduce the active surface area. As a result, CuO is often combined with oxides or other materials to reduce these drawbacks, improve its photocatalysis ability, and reduce the band gap [23]. Mamba et al. [24] reported that the use of Ag_2O as a single photocatalyst is limited due to its photosensitivity and rapid recombination of photoinduced e^-/h^+ pairs. Tariq et al. [25] prepared Ag_2O@CuO as a photocatalyst by the co-precipitation method to degrade the pesticide imidacloprid in a photocatalytic process. Introducing changes to the preparation procedures or precursors of the photocatalyst can significantly impact the properties of the produced photocatalyst. Herein, the Ag_2O@CuO heterojunction photocatalyst was prepared based on the same preparation procedures but using sodium hydroxide instead of ammonium bicarbonate to precipitate the Ag_2O@CuO heterojunction photocatalyst, and it will be used for degrading RhB dye as a model organic pollutant.

The present study focuses on the fabrication of Ag_2O@CuO heterojunction photocatalyst through the chemical co-precipitation method followed by calcination. The synthesized materials are employed for the photocatalytic degradation of RhB under UV light irradiation. The prepared photocatalyst will be characterized by X-ray diffraction, field emission scanning electron microscopy, X-ray fluorescence spectrometer, Fourier transform infrared spectroscopy, Ultraviolet–visible diffuse reflectance spectra, and photoluminescence spectroscopy. In addition, the influence of various operational parameters, including the light source, catalyst dosage, initial dye concentration, and solution pH, on the photocatalytic performance will be systematically investigated. Additionally, a kinetic study will be performed based on the experimental data of the oxidative photocatalytic degradation of RhB dye.

2- Experimental work

2.1. Martials

Cupric nitrate trihydrate ($Cu(NO_3)_2.3H_2O$, 95%) and silver nitrate ($AgNO_3$, 99%) were all obtained from LOBA CHEMIE PVT.LTD. Hydrochloric acid (HCl, 37 %) and sodium chloride (NaCl) were purchased from THOMAS BAKER. Sodium hydroxide (NaOH, 99 %) was purchased from Fisher Scientific. The RhB (MW = 479.02 g/mol) was provided by Central Drug House (New Delhi, India). Also, distilled water was used in all experiments.

2.2. Preparation of the photocatalyst

The co-precipitation method was utilized to prepare the Ag_2O@CuO heterojunction photocatalysts containing 5% of Ag_2O, as shown in Fig. 1. The preparation procedures of the heterojunction photocatalyst were made based on previous work conducted by Tariq et al. [25] with some manipulation. The photocatalyst was prepared by dissolving 5.78 g of copper nitrate in 50 mL of deionized water at 300 rpm for half an hour, then adding 0.147 g of silver nitrate to the copper nitrate solution until dissolved completely. 1 M of sodium hydroxide was added drop by drop to the above solution, and the pH was adjusted to 10, since no more precipitation occurred. The resulting black precipitate was collected and thoroughly washed with distilled water several times by centrifuging to remove residual sodium and nitrate ions. Finally, the precipitates

were dried for 2 h at 80 ℃, then calcined in a furnace at 400 ℃ for 2 h.

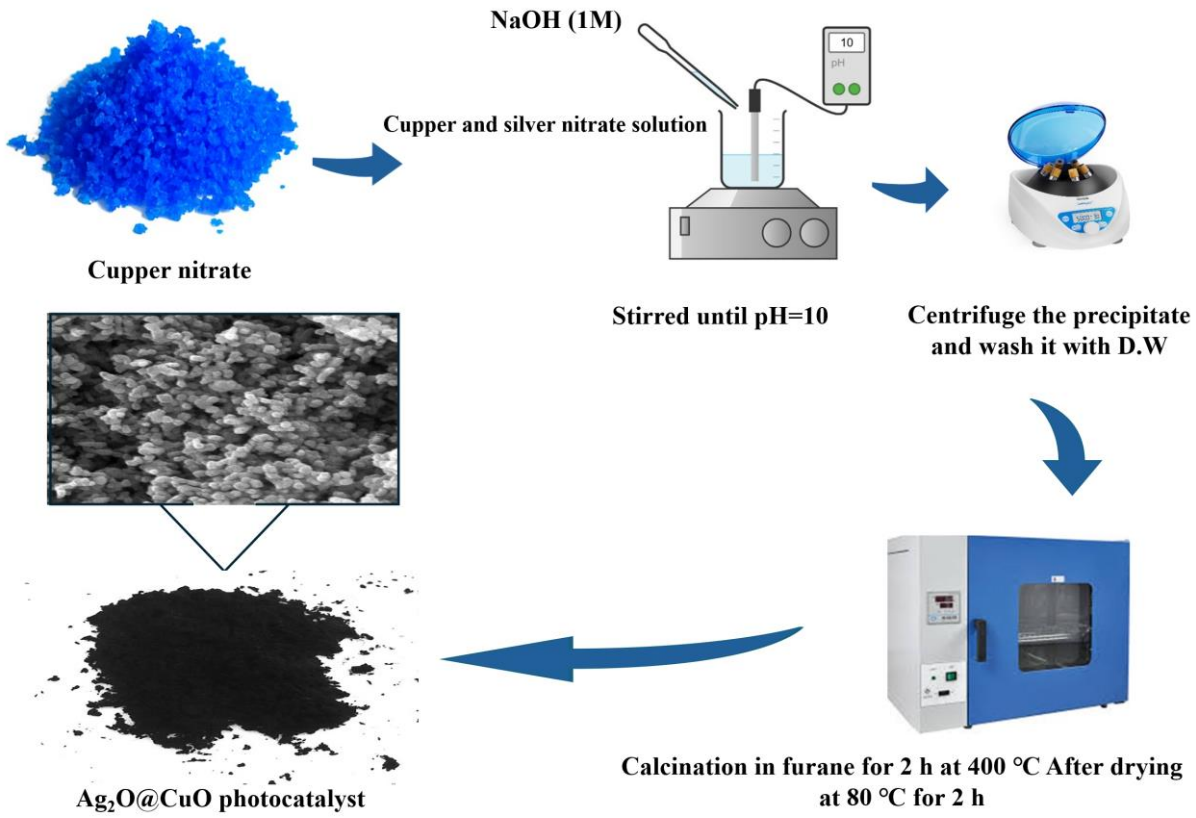

Fig. 1. Preparation of Ag_2O@CuO heterojunction photocatalyst

2.3. Characterization of the photocatalyst

The Ag_2O@CuO heterojunction photocatalyst was detected utilizing X-ray diffraction (XRD) by Malvern Panalytical with CuKα radiation (λ=1.5406) with a range of 2 Theta of 10º-80º. The composition of the Ag_2O@CuO photocatalyst was characterized using an X-ray fluorescence spectrometer (XRF spectrometer). Fourier-transform infrared spectrometer (FTIR) was used to detect the effective functional groups of the prepared heterojunction photocatalyst by an 1800IR spectrometer instrument in the range of 400-4000 cm^{-1}. Field emission scanning electron microscopy (FESEM, model Inspect TM F50) was used to examine the surface morphology of the Ag_2O@CuO photocatalyst. The Ultraviolet-Visible diffuse reflectance spectrometer (UV-Vis DRS, model Avantes-Avaspec-2048) was used to observe the optical properties of the synthesized Ag_2O@CuO heterojunction.

The Photoluminescence (PL) spectra of the catalyst were recorded using a Cary Eclipse fluorescence spectrometer. The point of zero-charge (pH_{pzc}) was studied for the Ag_2O@CuO heterojunction photocatalyst to examine its behavior towards RhB dye during the degradation process. The test was conducted by following the procedures mentioned in a published work [26]. The pH of a 0.1 M NaCl solution was initially set at 2, 4, 6, 7, 8, 10, and 12. After that, 100 mg of the phocatalyst was put in 50 mL of each solution above and shaken for 24 h. The pH was altered by a 0.1 M HCl solution and a 0.1 M NaOH solution. The pH recorded initially was subtracted from the pH recorded after 24 h, and the values were plotted against the initial pH. The pH_{pzc} was measured at the point where the curve intersects the X-axis.

2.4. Photocatalytic degradation of the RhB dye

The photocatalytic degradation of the RhB dye was studied using the Ag_2O@CuO heterojunction photocatalyst in a Pyrex beaker-type batch reactor in a dark mode, visible light supplied by two lamps of 50 W, and UV-C light irradiation supplied by four lamps of 8 W, as shown in Fig. 2. Different amounts of Ag_2O@CuO heterojunction photocatalyst (25, 50, 100, and 200 mg) were added to 100 mL of RhB dye solution (10 mg/L) and mixed (250 rpm) at room temperature. The samples were collected, centrifuged, and tested using a UV-Vis spectrophotometer at a wavelength of 546 nm. The photocatalytic degradation of RhB was examined by calculating the RhB degradation (%) given by Eq. 1.

$$\text{RhB degradation (\%)} = \frac{[RhB]_o - [RhB]_t}{[RhB]_o} * 100\% \quad (1)$$

That, $[RhB]_o$ is the initial concentration of the RhB dye (mg/L), $[RhB]_t$ is the RhB dye concentration (mg/L) at any time t (min).

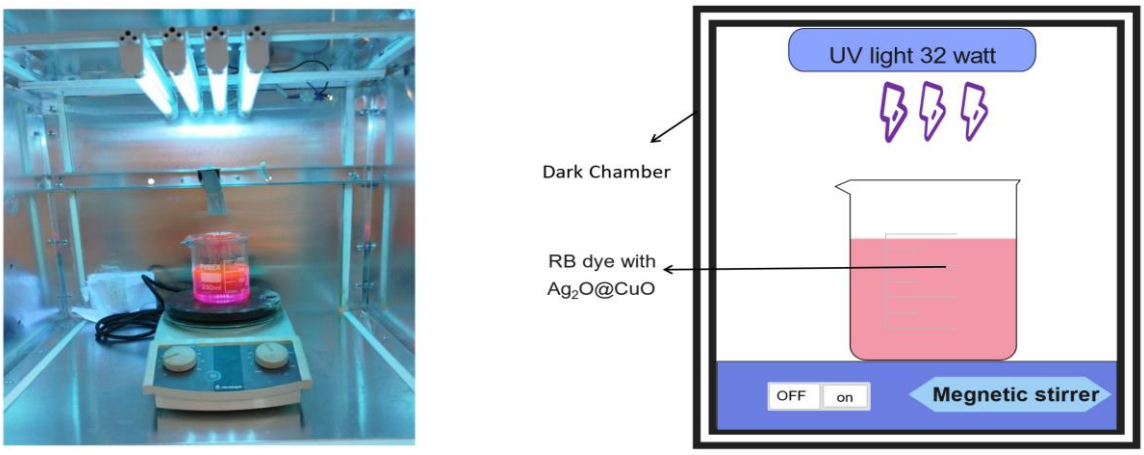

Fig. 2. Studying the activity of the Ag_2O@CuO photocatalyst in a batch setup

3- Result and discussion

3.1. Characterization of the photocatalyst

The chemical composition of the Ag_2O@CuO photocatalyst, given by the XRF analysis, is shown in Table 1. The results revealed that CuO is the main component of the Ag_2O@CuO photocatalyst, since it represented approximately 94.963 wt%; and the content of Ag_2O in the Ag_2O@CuO photocatalyst was 5.037%. These results agreed with those reported by Tariq et al. [25].

Table 1. The chemical analysis of the Ag_2O@CuO heterojunction photocatalyst by the XRF

Compositions, wt%	Ag_2O	CuO
Ag_2O@CuO	5.037	94.963

FT-IR was used to analyze the Ag_2O@CuO heterojunction photocatalyst for its functional group, and the spectra are shown in Fig. 3 (a). The peaks at 499.56 cm^{-1} and 596 cm^{-1} are related to the stretching vibration of the Cu-O bond in the monoclinic phase [27]. The stretching vibration of Ag-O-Ag bonds is shown by the low-intensity peak at 418.55 cm^{-1} [6, 15]. The peak observed at 1616 cm^{-1} is due to the bending vibrations of absorbed water molecules. The peak observed at 1382 cm^{-1} is attributed to the longitudinal phonon, which is similar to the character commonly possessed by nanoparticles [21, 24]. The peaks between 3417 cm^{-1} and 3477 cm^{-1} are related to the O–H bond of the hydroxyl functional group in water molecules that remain in the photocatalyst, similar to moisture [29].

The X-ray pattern of the Ag_2O@CuO photocatalyst was measured in the 2θ range of 10º-80º, as shown in Fig. 3 (b). The diffraction lines for CuO were found at 2θ of 32.45º, 35.53º, 38.7º, 46.21º, 48.712º, 51.33º, 53.35º, 58.23º, 61.47º, 66.06º, 67.96º, 72.35º, and 75.01º, which agreed well with standard diffraction values for monoclinic CuO with planes (111), (-111), (111), (-112), (-202), (112), (020), (202), (-113), (-311), (113), (311), and (-222), respectively; confirming the monoclinic crystal structure of CuO (JCPDS card No. 96-901-5925) [17, 20]. The distinctive diffraction peaks of Ag_2O were observed at 2θ of 29.30°,38.07°, 44.24°, 64.38°, and 77.33°. These peaks are associated with the Miller indices of (011), (111), (200), (220), and (311), respectively, which indicate the reflections of face-centered cubic (FCC) metal Ag (JCPDS card No. 87-0720 [26]). The average crystal size of the Ag_2O@CuO photocatalyst was estimated based on the XRD data using the Scherrer equation, shown in Eq. 2 [31]

$$D = \frac{K\lambda}{\beta \cos\theta} \quad (2)$$

Where D is the average crystal diameter (nm), λ is the X-ray wavelength of 1.5406 (Aº), β is the line diffraction broadening at FWHM (radian), and θ is the angle (degree). The average crystal size of the Ag_2O@CuO photocatalyst was estimated to be approximately 21.28 nm, which is consistent with the findings of Rahman et al. [32], who reported a value of 21.79 nm.

FESEM characterization was conducted to study the morphology of the Ag_2O@CuO heterojunction, that have an impact on the activity of the photocatalysts. Fig. 4 shows the morphology of the Ag_2O@CuO heterojunction as nanoellipsoidal particles. The average particle size of this photocatalyst was determined in the range of 26.27-56.85 nm.

The UV-Vis DRS spectra of the Ag_2O@CuO are shown in Fig. 5 (a) which displays that the highest absorption of Ag_2O@CuO heterojunction photocatalyst was between 200 and 312 nm. Eq. 3 was utilized to determine the bandgap energy (Eg) according to the Kubelka-Munk theory and Tauc's relation [33]:

$$(\alpha h\nu)^{1/n} = A(h\nu - Eg) \quad (3)$$

Where α represents the absorption coefficient, hv signifies the energy of the photon, and A represents the constant of proportionality. The calculated band gap of the Ag_2O@CuO heterojunction was 2.7 eV, which is

consistent with Vikal et al. [31] who reported that the band gap of CuO decreased as the amount of Ag_2O in a composite with CuO increased. Literature reported that CuO has a band gap of 2.5-3.5 eV, and it was identified by having a high recombination tendency [17, 27, 31, 34] and Ag_2O has a band gap of 1.2 eV [19]. Therefore, doping the CuO with 5% Ag_2O was successful in having a bandgap of 2.7 eV. The PL is performed to investigate the recombination behavior of the photogenerated charge carriers and to identify defect states within the semiconductor materials [35].

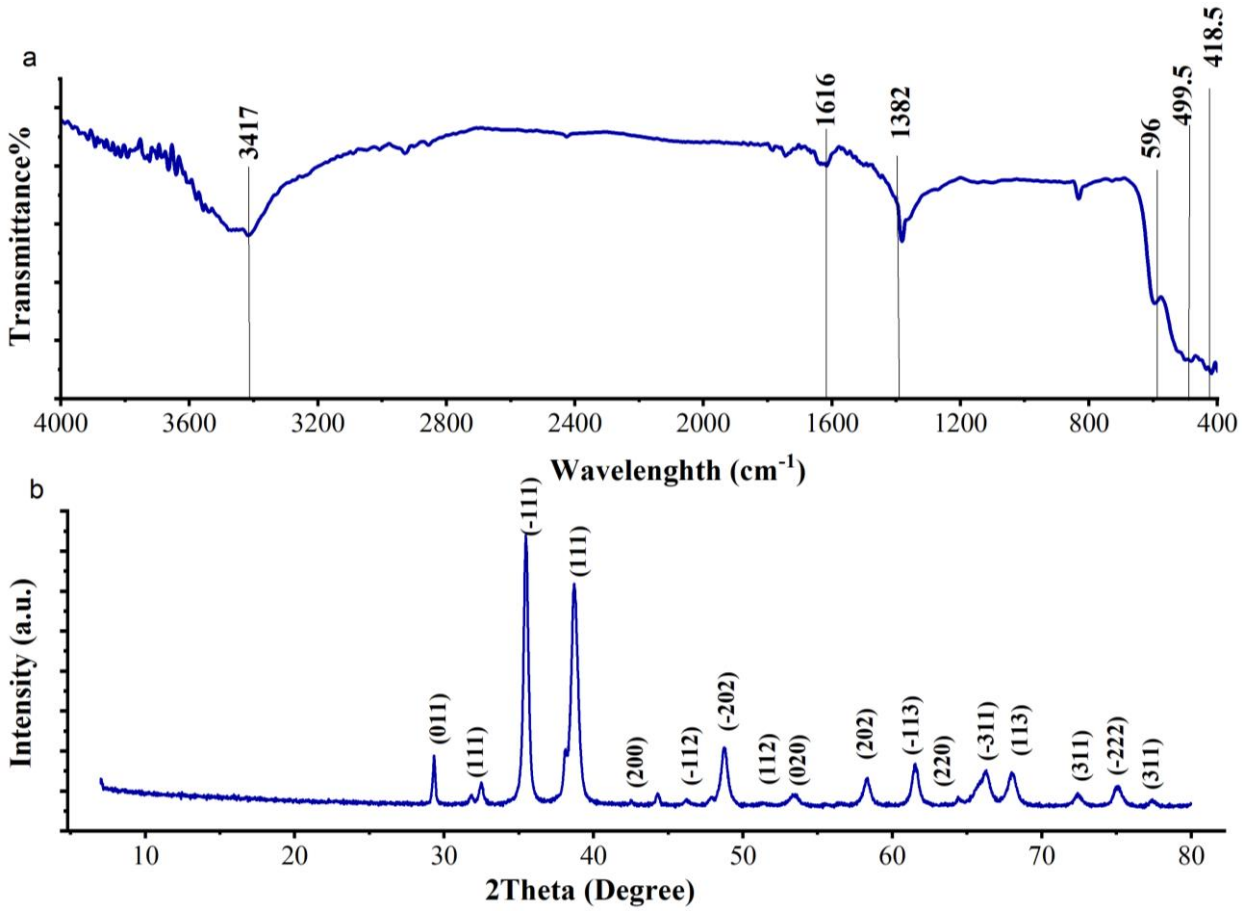

Fig. 3. The FT-IR spectra (a) and the XRD pattern (b) of the Ag_2O@CuO photocatalyst

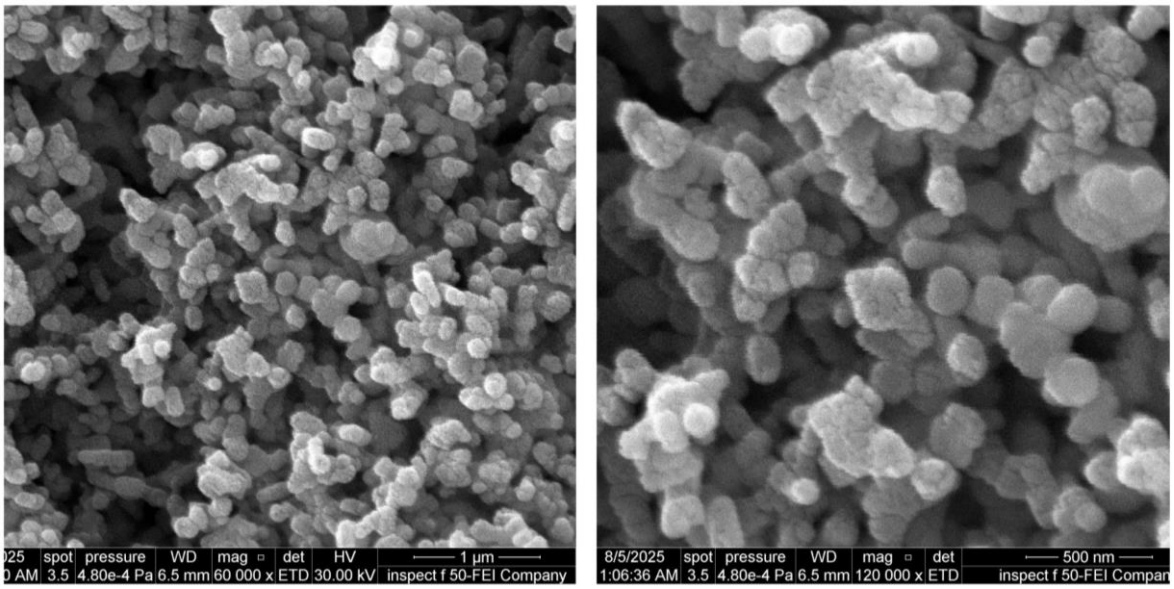

Fig. 4. The FESEM images of the Ag_2O@CuO heterojunction photocatalyst (scale bars of 1 µm and 500 nm)

The PL spectra of the Ag_2O@CuO heterojunction photocatalyst are shown in Fig. 5 (b) after excitation at 300 nm. There are two emission peaks that are observed at 355 nm (violet) and 480 nm (blue). The first one resulted from the band-edge emission. The second one originated from surface–related emissions or instrumental scattering effects. Notably, the intensity of PL decreased in the visible region (550-600 nm) compared to pristine CuO. This decrease leads to a reduction in the recombination rate of the e^-/h^+ pairs, resulting in effective separation of photogenerated charges [28-30].

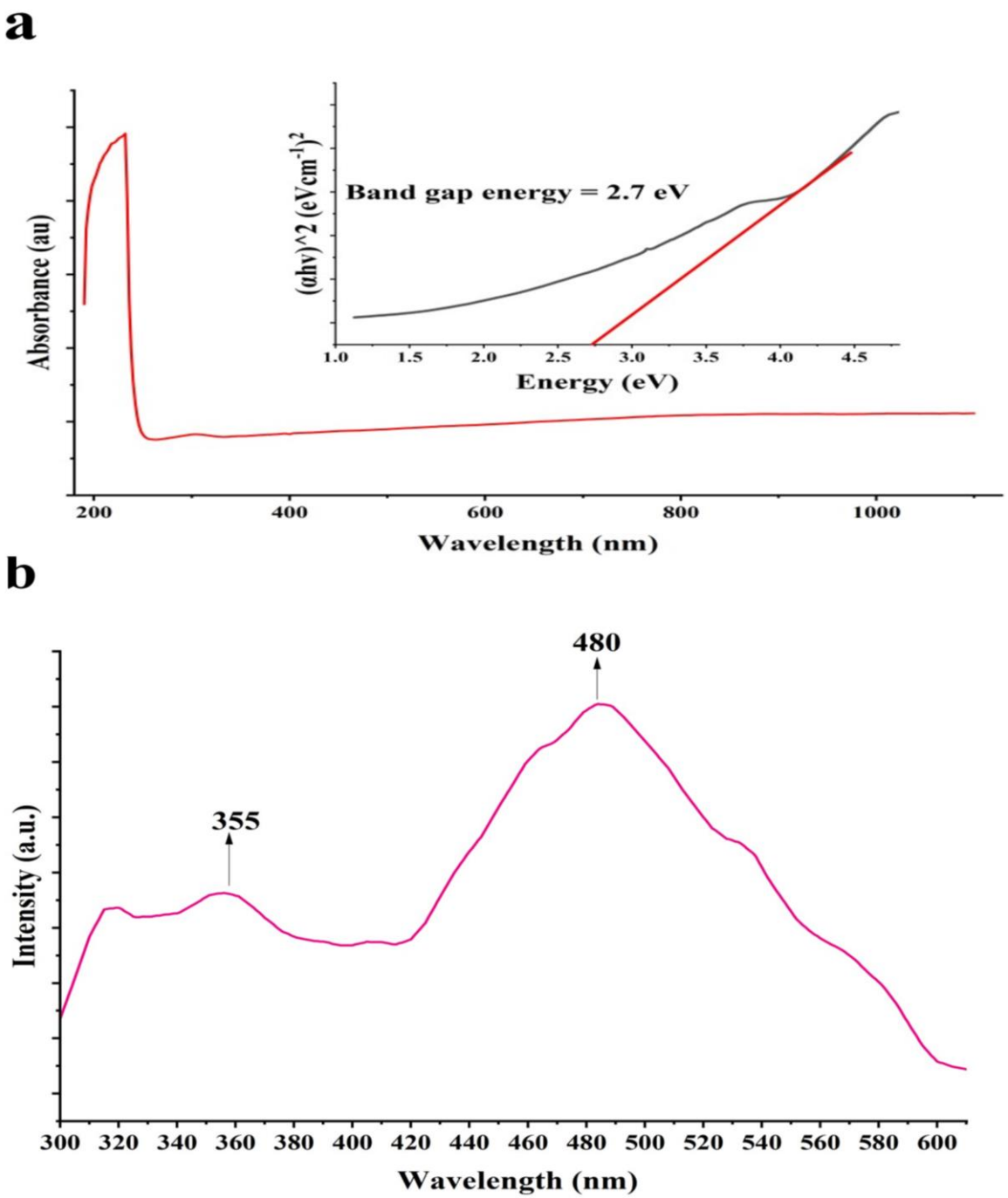

Fig. 5. The UV-Vis DRS spectra (a) and the PL spectra (b) of Ag_2O@CuO heterojunction photocatalyst

3.2. Effect of the Light Type on RhB Photocatalytic Degradation

The intensity of the supplied light affects the performance of the photocatalytic oxidation of pollutants [39]. Fig. 6 (a) shows the results of the photocatalytic degradation of RhB, which was studied at various light sources and conditions. The experiment was performed with fixed parameters, involving the dosage of the photocatalyst of 50 mg/100 mL, initial RhB concentration of 10 mg/L, pH of 6.8, and the reaction time of 90 min. The experiment was performed at different conditions involving dark, visible light (two lamps, each 50 W), and UV light (four UV-C lights, 32 W). The RhB dye was

exposed to direct UV irradiation without a photocatalyst under the same fixed parameters above, and only about 1.4% degradation of RhB was obtained after 90 minutes. Also, the results showed that the degradation of RhB using Ag_2O@CuO heterojunction photocatalyst was 18% in the dark. Moreover, under identical conditions in visible light, the removal gradually increased over time to reach 30.41% after 90 min of degradation. However, the placement of UV light led to a notable increase in the photocatalysis degradation of the RhB dye throughout the reaction duration, reaching 91% after 90 min. These results can be explained as that dark conditions and visible light did not provide enough energy to excite the electrons; therefore, low degradation was obtained. Conversely, UV light supplied sufficient energy to excite electrons in the photocatalyst, enabling the production of reactive species $^{\bullet}OH$, $\bullet O_2^-$, e^-, and h^+ that contribute to breaking down the RhB dye. The same results were obtained by Vengatakrishnan et al. [40].

3.3. Effect of the photocatalyst dose on RhB photocatalytic degradation.

The influence of the Ag_2O@CuO heterojunction photocatalyst dose on the photocatalytic degradation of RhB dye was studied at an initial RhB concentration of 10 mg/L, pH of 6.8, and the Ag_2O@CuO catalyst dosages of 25–200 mg/100 mL. Fig. 6 (b) shows the photocatalytic degradation efficiency for the RhB under UV irradiation at different photocatalyst doses. This figure shows that the photocatalytic degradation increased with reaction time for all doses. The extent of degradation was significantly dependent on the photocatalyst dose. The photocatalyst showed the highest degradation of RhB (approximately 90.5%) at a minimal loading of 50 mg, after 90 min of starting reaction time.

When the dose was 25 mg, the degradation was 85.12% for the RhB. This obviously enhanced degradation can be attributed to the generation of sufficient reactive species for RhB degradation, since UV irradiation can efficiently create e^-/h^+ pairs, which enhances the generation of reactive species such as h^+, $^{\bullet}OH^-$, e^-, and $^{\bullet}O_2^-$, that degrade the molecules of the RhB [41]. Notably, the degradation was reduced by increasing the dose of the photocatalyst until reaching nearly 75% at 100 mg/100 mL. Whilst at a high photocatalyst dose (200 mg), the degradation exhibited lower degradation efficiency (38.5%) at the same reaction time. This is because the particles of the photocatalyst cause light scattering and shielding effects that lead to a decrease in photon penetration. In addition to that, at higher concentrations of dose, there is a large chance for the generation of more agglomeration of nanoparticles, which leads to decreased surface area and blocked active sites [42].

3.4. Effect of pH of the dye solution

The pH of the solution is an essential factor in the photocatalytic degradation of organic pollutants, since it influences the charge of the catalyst surface throughout the process. This study was performed at an initial RhB concentration of 10 mg/L, Ag_2O@CuO heterojunction photocatalyst dose of 50 g/100 mL, reaction time of 90 min, and UV light irradiation. Fig. 8 (a) shows a significant enhancement in the degradation of RhB dye when using the Ag_2O@CuO heterojunction photocatalyst as the pH of the RhB dye solution increased from 4 to 10, with a markedly high degradation efficiency at pH 10 compared to pH 4.

The results show that the photocatalytic degradation of the RhB was nearly 97.23% at a pH of the RhB solution of 10 after 90 min. On the other hand, at a pH of 4, the degradation occurred slowly until reaching 28.16% after 90 min. The RhB dye has pK_a of 3.7-4.3. pK_a measures the acidity of the molecule. At $pK_a \leq 3.7$, the RhB is protonated, and a zwitterion (has both negative and positive charges) when pK_a 3.7-4.3. When the pH is 3, the RhB presents as a protonated molecule (cationic RhB+). However, RhB evolves from a cationic to a zwitterionic state at pH = 5 because of the deprotonation of its COOH groups [43]. Consequently, the cationic RhB dye (RhB+) predominates in the solution. The pH_{pzc} of the Ag_2O@CuO photocatalyst was 6.1, as presented in Fig. 7. When the solution pH exceeded the pH_{pzc}, the Ag_2O@CuO photocatalyst surface acquired a negative charge, hence attracting RhB+. At a solution pH below the pH_{pzc}, the Ag_2O@CuO surface exhibited a positive charge, repelling RhB+.

3.5. Effect of the initial RhB concentration

The photocatalytic degradation of RhB dye was examined using a photocatalyst dose of 50 mg/100 mL, at an initial RhB concentration range (5-15 mg/L), with a reaction time of 90 min, a pH of 6.8, and under UV light irradiation. The outcomes are shown in Fig. 8 (b). The results show that at an initial RhB concentration of 5 mg/L, the RhB photocatalytic degradation efficiency reached about 98% in 90 min. This means that almost all the RhB was mineralized under UV light in the presence of Ag_2O@CuO heterojunction photocatalyst. The degradation continued with an 86% degradation efficiency at a concentration of 15 mg/L of RhB.

The reduction in the degradation efficiency when the concentration of RhB increased can be explained by two reasons. Firstly, as the concentration of RhB increased, the solution color inhibited light penetration, and thus weak generation of e^-/h^+ pairs. Secondly, the reactive species ($^{\bullet}OH^-$ and $^{\bullet}O_2^-$) produced by a certain dose of the photocatalyst were not enough for the decomposition of a larger number of dye molecules. Nevertheless, the photocatalytic degradation efficiency of the RhB remained around 90% even with increasing initial concentration of RhB, demonstrating the strong photocatalytic activity and stability of the prepared heterojunction photocatalyst, suggesting its potential use in real wastewater applications. Similar results were obtained by Chong et al. [41].

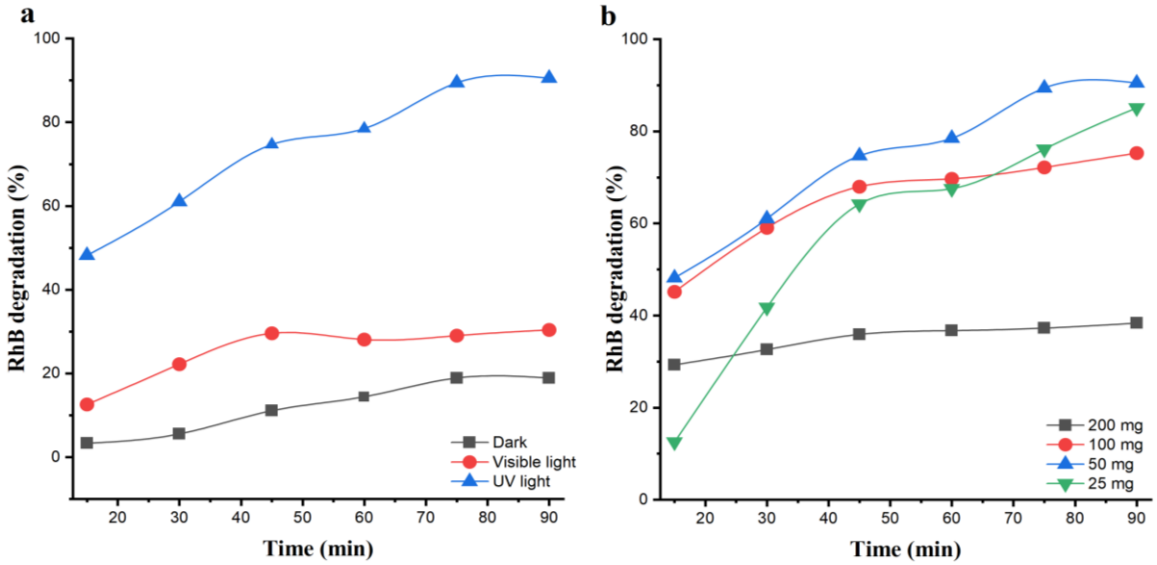

Fig. 6. Effect of light type (a) and Effect of Ag_2O@CuO photocatalyst dose (b) on the photocatalytic degradation of the RhB dye

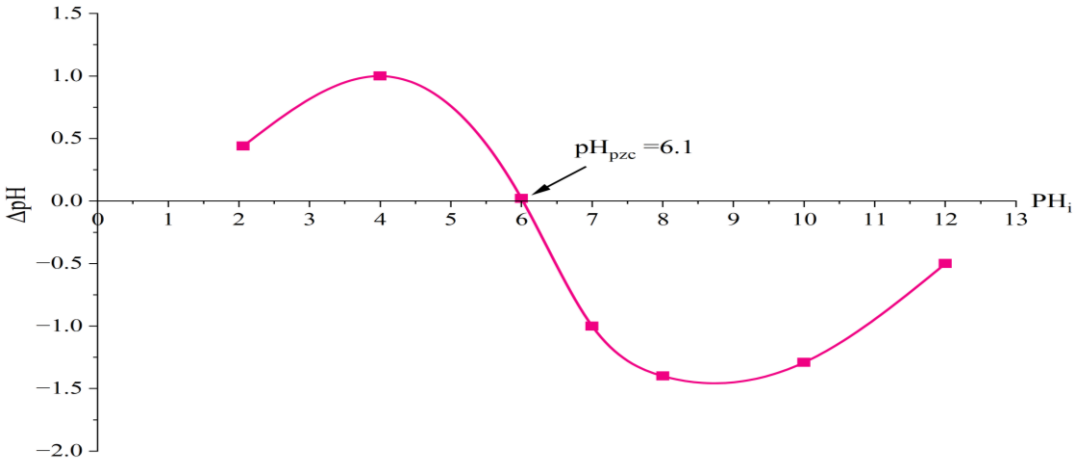

Fig. 7. Surface charge of Ag_2O@CuO photocatalyst

4- The photocatalysis reaction kinetics

The kinetic model of RhB photocatalytic degradation was evaluated by curve fitting with the zero-order, pseudo-first order, and modified Freundlich models. The mathematical expressions of the applied kinetic models are represented in Eqs. 4-6 corresponding to the zero-order, pseudo-first order, and modified Freundlich order, respectively. The linearized form of the modified Freundlich model is given by Eq. 7 [44-46].

$$C_{RhBo} - C_{RhBt} = k_0 t \quad (4)$$

$$\ln(C_{RhBo}/C_{RhBt}) = k_1 . t \quad (5)$$

$$C_{RhBt} = k_{Fr} . C_{RhBo} . t^{1/m} \quad (6)$$

$$\ln(C_{RhBt}) = \ln(k_{Fr} . C_{RhBo}) + (1/m)\ln(t) \quad (7)$$

Where k_o (mg/L.min), k_1 (min^{-1}), and k_{Fr} (min^{-1}/m) are the apparent constants of the zero-order, pseudo-first order, and modified Freundlich models, respectively. m is the modified Freundlich exponent. Fig. 9 presents the plots of the kinetic models for the photocatalytic degradation of the RhB dye utilizing the Ag_2O@CuO heterojunction photocatalyst.

An accurate comparison using correlation coefficients (R^2) values showd that the pseudo-first order model was the best fitted with the photocatalytic oxidation data of the RhB than the other models. The Langmuir Hinshelwood kinetic model (Eq. 8) describes the relationship between the initial pollutant concentration and the photocatalytic degradation rate [47].

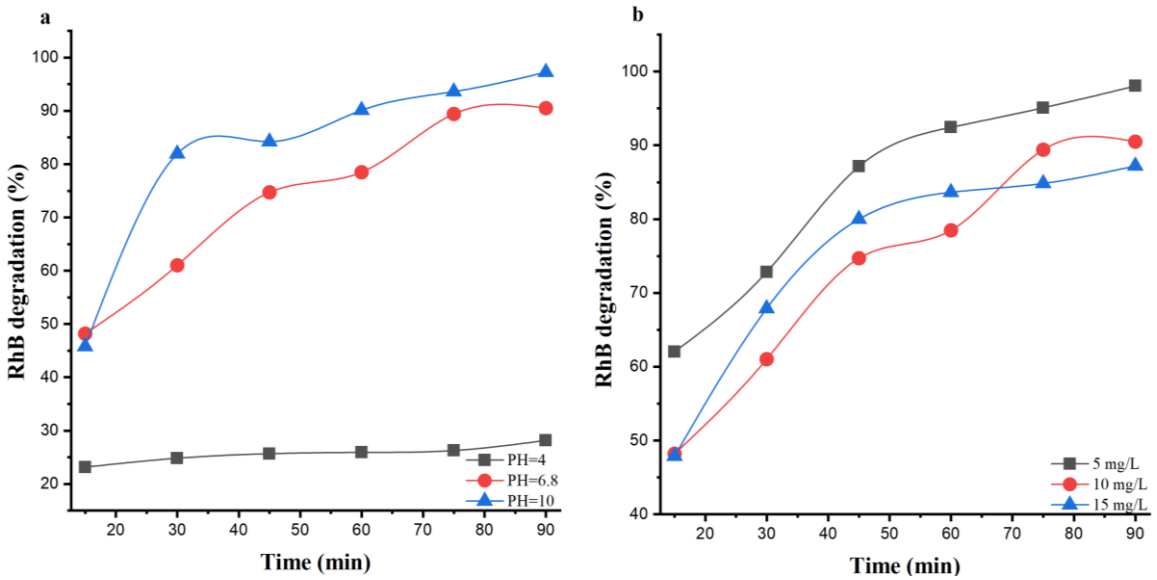

Fig. 8. Effect of the RhB dye solution pH (a) and Effect of initial RhB concentration (b) on the photocatalytic degradation of the RhB dye

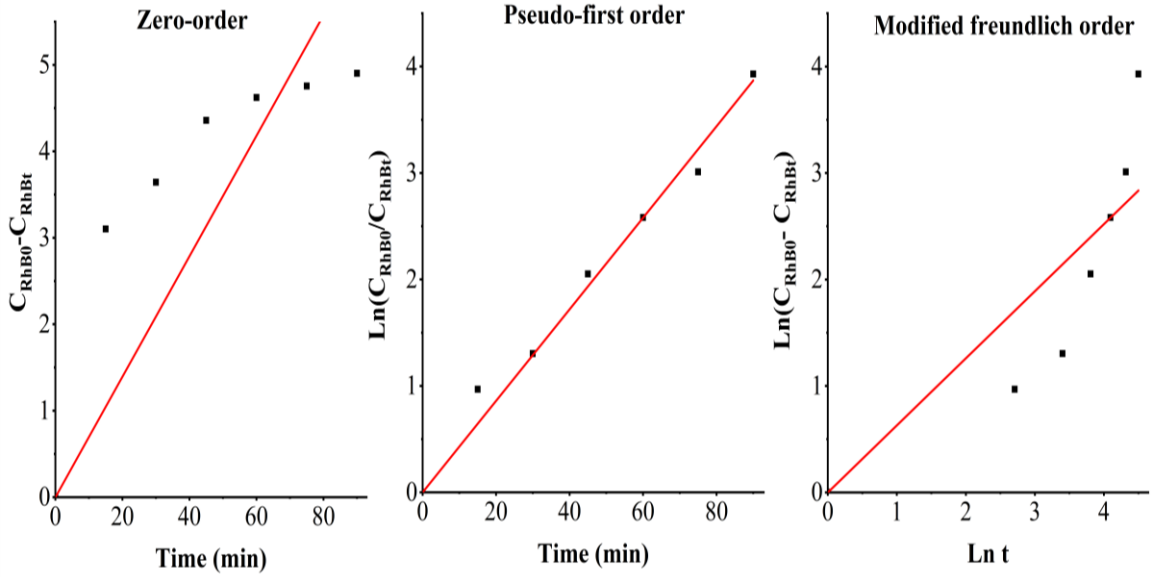

Fig. 9. The plots of fitting the kinetic models for the photocatalytic degradation of the RhB dye by Ag_2O@CuO photocatalyst

Table 2. The determined parameters of the kinetic models used for studying the photocatalytic degradation of the RhB dye

Kinetics model	Model parameters and R^2	
Zero-order	k_0 (mg/L.min)	0.0696
	R^2	0.9051
Pseudo-first order	k_1 (min^{-1})	0.0429
	R^2	0.9955
Modified Freundlich	k_{Fr} (min^{-1})	0.6300
	R^2	0.9302

$$r_{RhB} = -dC_{RhB}/dt = (k_r K_{ad}/(1 + K_{ad} C_{RhB0})) C_{RhB}^{n} \quad (8)$$

Where k_r represents the actual photocatalysis reaction rate constant (mg/L.min) and K_{ad} represents the Langmuir-Hinshelwood constant of adsorption (L/mg). Ćelić et al. [48], assumed pseudo-first order reaction kinetics to resolve Eq. 8.

Chakachaka et al. [45], reduced Eq. 8 to Eq. 9 by considering a minimal initial concentration of the targeted pollutant; thus, the response rate will depend on reaction time rather than the pollutant concentration.

$$r_{RhB} = k_r . K_{ad} . C_{RhB} \quad (9)$$

As the obtained results indicated that the reaction rate of the RhB photocatalytic degradation over the Ag_2O@CuO photocatalyst follows the pseudo-first order kinetics, the value of n in Eq. 8 will be set as 1, which will result in Eq. 10 [49].

$$r_{RhB} = k_1 . C_{RhB} \quad (10)$$

$$k_1 = k_r\, K_{ad}./\,(1 + K_{ad}.C_{RhB0}) \quad (11)$$

$$\frac{1}{k_1} = \frac{1}{k_r K_{ad}} + \left(\frac{1}{k_r}\right) C_{RhB0} \quad (12)$$

The values of k_r and K_{ad} are shown in Eq.12 can be estimated by a linear plot of $\frac{1}{k_1}$ vers C_{RhB0}.

Table 3 shows that the apparent rate constant decreased with increasing the initial RhB concentration, thereby reducing photocatalytic performance. This can be attributed to the high pollutant concentrations, which slow down the photocatalytic degradation rate because they affect the solution's turbidity, causing absorption of light by pollutants instead of the photocatalyst. These results are consistent with Adday et al. [49]. Additionally, Table 3 presents the value of k_r of 0.7184 mg/L.min and the value of K_{ad} of 0.0767 L/mg. This result demonstrates the high potential of the prepared Ag_2O@CuO heterojunction photocatalyst for degrading the RhB dye under UV light irradiation than its adsorption capacity.

Table 3. The apparent rate constant and the Langmuir-Hinshelwood model constants of the RhB photocatalytic degradation by Ag_2O@CuO heterojunction photocatalyst

Initial RhB dye concentration (mg/L)	Ag_2O@CuO heterojunction photocatalyst	
	k_1 (min^{-1})	R^2
5	0.043	0.9956
10	0.028	0.9908
15	0.0269	0.9664
	k_r = 0.7184 mg/L.min $K_{ad.}$ = 0.0767 L/mg	

5- Conclusion

The Ag_2O@CuO heterojunction photocatalyst was synthesized by a co-precipitation method. The photocatalytic performance of the prepared catalyst was investigated in the RhB photocatalytic degradation and characterized by XRF, XRD, FT-IR, UV-Vis DRS, PL, and FESEM. The Ag_2O@CuO photocatalyst had an average crystal size of 21.28 nm. The photocatalytic activity results demonstrated that at neutral pH and using UV light, the Ag_2O@CuO photocatalyst showed a high degradation of RhB of 91% after 90 min. The solution pH was the most influential parameter in the RhB degradation process.

The highest degradation of RhB dye concentration of 10 mg/L, Ag_2O@CuO photocatalyst dose of 50 mg/100 mL, pH of 10, and reaction time of 90 min. Also, the kinetic study was performed based on the experimental data of the oxidative photocatalytic degradation of the RhB dye. The results showed that the photocatalytic oxidation of RhB dye by the Ag_2O@CuO heterojunction photocatalyst followed a pseudo-first order kinetic model, with an apparent rate constant of 0.0429 min^{-1}. Additionally, applying the Langmuir-Hinshelwood model showed that the intrinsic photocatalysis reaction rate constant was 0.7184 mg/L.min and the equilibrium adsorption constant was 0.0767 L/mg. This study underscores the high potential of the prepared photocatalyst for eliminating the organic dyes from water.

References

[1] S.Fatima, M.Iqpal, H.N. Bhatti, M. Iqbal, N. Alwadai, "Synthesis of Oval-Shaped Bi2Al4O9 Nanoparticles and Their Applications for the Degradation of Acid Green 25 and as Fuel Additives,"*ACS Omega*, vol. 8, no. 34, pp. 30868–30878, Aug. 2023, Accessed: Dec. 03, 2025. https://doi.org/10.1021/acsomega.3c01245

[2] A. G. Saleem, S. M. Al-Jubouri, S. Al-Batty, M. Wali Hakami, "Determination of controlling fouling mechanism using the Hermia models and estimation of the manufacturing costs of the modified polyvinylidene fluoride-based ultrafiltration membranes," *Iraqi Journal of Chemical and Petroleum Engineering*, vol. 26, no. 1, pp. 67–76, Mar. 2025, https://doi.org/10.31699/IJCPE.2025.1.7

[3] Q. Reza, I. Bibi, F. Majid, S. Kamal, S.Ata, A.Ghafoor, M.I.Arshad, S. Al-Mijalli, A. Nazir, M. Iqbal, "Solar light-based photocatalytic removal of CV and RhB dyes using Bi and Al doped SrFe12O19 NPs and antibacterial properties," *Journal of Industrial and Engineering Chemistry*, vol. 118, pp. 469–482, 2023, https://doi.org/10.1016/j.jiec.2022.11.030

[4] A.G. Saleem and S.M. Al-Jubouri, "Separation performance of cationic and anionic dyes from water using polyvinylidene fluoride-based ultrafiltration membrane incorporating polyethylene glycol," *Desalination and Water Treatment*, vol. 319, Jul. 2024, https://doi.org/10.1016/j.dwt.2024.100546

[5] A.G. Saleem and S. M. Al-Jubouri, "Efficient Separation of Organic Dyes using Polyvinylidene Fluoride/Polyethylene Glycol-Tin Oxide (PVDF/PEG-SnO2) Nanoparticles Ultrafiltration Membrane," *Applied Science and Engineering Progress*, vol. 17, Oct. 2024, https://dx.doi.org/10.14416/j.asep.2024.08.001

[6] A.B. Salman, "Electrochemical oxidation of methyl orange dye by stainless steel rotating cylinder anode," *International Journal of Environment and Waste Management*, vol. 28, p. 114, Jan. 2021, https://doi.org/10.1504/IJEWM.2021.117012

[7] A.S. Adday and S. M. Al-Jubouri, "Developing a versatile visible-light-driven polyvinylidene fluoride/Ag2O@CRA photocatalytic membrane for efficient treatment of organic pollutants-contained wastewater," *Journal of Water Process Engineering*, vol. 73, May 2025, https://doi.org/10.1016/j.jwpe.2025.107713

[8] T.D. Kusworo, M. Yulfarida, A.C. Kumoro, S.Sumardiono, M.Djaeni, T.A. Kurniawan, M.H.D. Othman, B. Budiyono, "A highly durable and hydrophilic PVDF- MoS2/WO3-PVA membrane with visible light driven self-cleaning performance for pollutant-burdened natural rubber wastewater treatment," *Journal of Environmental Chemical Engineering*, vol. 11, no. 2, Apr. 2023, https://doi.org/10.1016/j.jece.2023.109583

[9] N.A. Mohammed, A.I. Alwared, M.S. Salman, "Photocatalytic Degradation of Reactive Yellow Dye in Wastewater using H2O2/TiO2/UV Technique, " *Iraqi Journal of Chemical and Petroleum Engineering*, vol. 21, no. 1, pp. 15–21, Mar. 2020, https://doi.org/10.31699/IJCPE.2020.1.3

[10] G. Viswanathan, A. Solaiappan, B. Thirumalairaj, U. Krishnamoorthy, N. Lakeshmaiya, M.I.H. Siddiqui, M.S. Shan, "Improved photocatalytic properties of WO3 nanoparticles for Malachite green dye degradation under visible light irradiation: An effect of la doping," *Open Chemistry*, vol. 22, no. 1, Jan. 2024, https://doi.org/10.1515/chem-2024-0035

[11] M. Pirhashemi, A. Habibi-Yangjeh, S.R. Pouran, "Review on the criteria anticipated for the fabrication of highly efficient ZnO-based visible-light-driven photocatalysts," *Korean Society of Industrial Engineering Chemistry*, Jun. 25, 2018, https://doi.org/10.1016/j.jiec.2018.01.012

[12] O. Długosz and M. Banach, "Morphology and photocatalytic properties of Ag2O nanoparticles synthesised in processes based on different forms of energy," *Journal of Cleaner Production*, vol. 415, p. 137733, 2023, https://doi.org/10.1016/j.jclepro.2023.137733

[13] S. Singla, S. Sharma,S. Basu, "MoS2/WO3 heterojunction with the intensified photocatalytic performance for decomposition of organic pollutants under the broad array of solar light," *Journal of Cleaner Production*, vol. 324, p. 129290, 2021, https://doi.org/10.1016/j.jclepro.2021.129290

[14] P. Raizada, A. Sudhaik, S. Patial, V. Hasija, A.A.P. Khan, P.S.S. Gautam, M. Kaur, V. Nguyen, "Engineering nanostructures of CuO-based photocatalysts for water treatment: Current progress and future challenges," *Arabian Journal of Chemistry*, vol. 13, no. 11, pp. 8424–8457, Nov. 2020, https://doi.org/10.1016/j.arabjc.2020.06.031

[15] S.I. Siddiqui, M. Naushad, S.A. Chaudhry, "Promising prospects of nanomaterials for arsenic water remediation: A comprehensive review," *Institution of Chemical Engineers, Official Journal of the European Federation of Chemical Engineering: Part B,* Jun. 01, 2019, https://doi.org/10.1016/j.psep.2019.03.037

[16] J. Guo, N. Akram, L. Zhang, W.M.G. Wang, Y. Zhang, A.Ahmad, J. wang, "Ag2O modified CuO nanosheets as efficient difunctional water oxidation catalysts," *Journal of Photochemistry and Photobiology A: Chemistry*, vol. 433, p. 114166, 2022, https://doi.org/10.1016/j.jphotochem.2022.114166

[17] A. Bajwa, H. Kaur, S. Kumar, G. Singh, "Excitation-wavelength-dependent photoluminescence/electrical conductivity of copper oxide nanorods," *Surface Innovations*, vol. 12, no. 5, pp. 300–308, 2024, https://doi.org/10.1680/jsuin.23.00056

[18] T. Iqbal, A. Masood, N.R. Khalid, M.B. Tahir, A.M. Asiri, H. Alrobei, "Green synthesis of novel lanthanum doped copper oxide nanoparticles for photocatalytic application: Correlation between experiment and COMSOL simulation," *Ceramics International*, vol. 48, no. 10, pp. 13420–13430, 2022, https://doi.org/10.1016/j.ceramint.2022.01.160

[19] W.M. Shume, H.C.A. Murthy, E.A. Zereffa, "A Review on Synthesis and Characterization of Ag2O Nanoparticles for Photocatalytic Applications," *Journal of Chemistry*, 2020, https://doi.org/10.1155/2020/5039479

[20] W.Al-Zoha, O. Hussien, A. Iftikhar, F.Aziz, D. Alhashmialameer, S. Mahmoud, M.F. Warsi, D. saleh, "Co-precipitation assisted preparation of Ag2O, CuO and Ag2O/CuO nanocomposite: Characterization and improved solar irradiated degradation of colored and colourless organic effluents," *Ceramics International*, vol. 48, no. 13, pp. 19056–19067, 2022, https://doi.org/10.1016/j.ceramint.2022.03.194

[21] A. Alsulmi, N.N. Mohammed, A. Soltan, M.F.A. Messih, M.A. Ahmed, "Engineering S-scheme CuO/ZnO heterojunctions sonochemically for eradicating RhB dye from wastewater under solar radiation," *RSC Advances*, vol. 13, no. 19, pp. 13269–13281, Apr. 2023, https://doi.org/10.1039/D3RA00924F

[22] A.K. Sibhatu, G.K. Weldegebrieal, S. Sagadevan, N.N. Tran, V. Hessel, "Photocatalytic activity of CuO nanoparticles for organic and inorganic pollutants removal in wastewater remediation," *Chemosphere*, vol. 300, p. 134623, 2022, https://doi.org/10.1016/j.chemosphere.2022.134623

[23] S.D. Roy, K.C. Das, S.S. Dhar, "Facile synthesis of CuO-Ag2O hybrid metal oxide composite using carica papaya, cocooning with hydroxyapatite, and photocatalytic degradation of organic dyes," *Materials Science and Engineering: B*, vol. 303, p. 117331, 2024, https://doi.org/10.1016/j.mseb.2024.117331

[24] F.B. Mamba, B.S. Mbuli, J. Ramontja, "Synergistic effect of ZnO/Ag2O@g-C3N4 based nanocomposites embedded in carrageenan matrix for dye degradation in water," *Heliyon*, vol. 10, no. 11, Jun. 2024, https://doi.org/10.1016/j.heliyon.2024.e31109

[25] S.R. Tariq, Z. Niaz, G.A. Chotana, D. Ahmad, N. Rafique, "Photocatalytic degradation of imidacloprid using Ag2O/CuO composites," *RSC Advance*, vol. 13, no. 28, pp. 19326–19334, Jun. 2023, https://doi.org/10.1039/D3RA02109B

[26] A.S. Adday and S.M. Al-Jubouri, "Photocatalytic oxidative removal of the organic pollutant from wastewater using recyclable Ag2O@CRA heterojunction photocatalyst," *Case Studies in Chemical and Environmental Engineering*, vol. 10, Dec. 2024, https://doi.org/10.1016/j.cscee.2024.100852

[27] H. Saha, A. Dastider, J.F. Anik, S.R. Mim, S. Talapatra, U. Das, M. Jamal, M. Billah, "Photocatalytic performance of CuO NPs: An experimental approach for process parameter optimization for Rh B dye," *Results in Materials*, vol. 24, Dec. 2024, https://doi.org/10.1016/j.rinma.2024.100614

[28] R.S. Ganesh, M. Navaneethan, V.L.Patil, S. Ponnusamy, C.Muthamizhchelvan, S. Kawasaki, P.S. Patil, Y. Hayakama, "Sensitivity enhancement of ammonia gas sensor based on Ag/ZnO flower and nanoellipsoids at low temperature," *Sensors and actuators B: Chemical, Actuators B Chem*, vol. 255, pp. 672–683, 2018, https://doi.org/10.1016/j.snb.2017.08.015

[29] R.T. Yunarti, I.D. Isa, L.C.C. Dimonti, A. A. Dwiatmoko, M. Ridwan, J.M. Ha, "Study of Ag2O/TiO2 nanowires synthesis and characterization for heterogeneous reduction reaction catalysis of 4-nitrophenol," *Nano-Structures and Nano-Objects*, vol. 26, Apr. 2021, https://doi.org/10.1016/j.nanoso.2021.100719

[30] T. Saha, M. Bin Mobarak, M.N. Uddin, M.S. Quddus, M.R. Naim, N.S. Pinky, "Biogenic synthesis of copper oxide (CuO) NPs exploiting Averrhoa carambola leaf extract and its potential antibacterial activity," *Materials Chemistry and Physics*, vol. 305, p. 127979, 2023, https://doi.org/10.1016/j.matchemphys.2023.127979

[31] S. Vikal, Y. Gautam, A. Kumar, A. Kumar, N. Singh, H. Singh, B. singh, "Effect of silver (Ag) doping on structural, optical and antimicrobial properties of copper oxide (CuO) nanostructures," *Nano Express*, vol. 4, no. 2, Jun. 2023, https://doi.org/10.1088/2632-959X/acdc41

[32] M.M. Rahman, M.M. Alam, M.M. Hussain, A.M. Asiri, M.E.M. Zayed, "Hydrothermally prepared Ag2O/CuO nanomaterial for an efficient chemical sensor development for environmental remediation," *Environmental Nanotechnology, Monitoring and Management*, vol. 10, pp. 1–9, Dec. 2018, https://doi.org/10.1016/j.enmm.2018.04.001

[33] N. Alomayrah, M. Ikram, S. Zulfiqar, S. Alomairy, M.S. Al-Buriahi, I. Shakir, M.F. Warsi, E.W. Cochran, "Fabrication of a highly efficient CuO/ZnCo2O4/CNTs ternary composite for photocatalytic degradation of hazardous pollutants," *RSC Advances*, vol. 14, no. 34, pp. 24874–24897, Aug. 2024, https://doi.org/10.1039/D4RA04395B

[34] M.U.Khalid, M.F. Warsi, M.I. Sarwar, P.O. Agboola, I. Shakir, S. Zulfiqar, "Visible light driven photocatalytic activity of unsubstituted and Ag1+ / Al3+-substituted CuO nanoflakes," *Ceramics International*, vol. 46, no. 9, pp. 14287–14298, 2020, https://doi.org/10.1016/j.ceramint.2020.02.211

[35] S. Liang, D. Zhang, X. Pu, X. Yao, R. Han, J. Yin, X. Ren, "A novel Ag2O/g-C3N4 p-n heterojunction photocatalysts with enhanced visible and near-infrared light activity," *Separation and Purification Technology*, vol. 210, pp. 786–797, 2019, https://doi.org/10.1016/j.seppur.2018.09.008

[36] A.A. Menazea and A.M. Mostafa, "Ag doped CuO thin film prepared via pulsed laser deposition for 4-nitrophenol degradation," *Journal Environmental Chemical Engineering*, vol. 8, no. 5, Oct. 2020, https://doi.org/10.1016/j.jece.2020.104104

[37] C. Tamuly, I. Saikia, M. Hazarika, M.R. Das, "Reduction of aromatic nitro compounds catalyzed by biogenic CuO nanoparticles," *RSC Advances*, vol. 4, no. 95, pp. 53229–53236, 2014, https://doi.org/10.1039/C4RA10397A

[38] N.D. Khiavi, R. Katal, S.K. Eshkalak, S. Masudy-Panah, S. Ramakrishna, H. Jiangyong, "Visible light driven heterojunction photocatalyst of cuo-cu2o thin films for photocatalytic degradation of organic pollutants," *Nanomaterials*, vol. 9, no. 7, Jul. 2019, https://doi.org/10.3390/nano9071011

[39] Z. Guo, D. Kodikara, L.S. Albi, Y. Hatano, G. Chen, C. Yoshimura, J. Wang, "Photodegradation of Organic Micropollutants in Aquatic Environment: Importance, Factors and Processes," *Water Research*, vol. 231, p. 118236, Mar. 2023, https://doi.org/10.1016/j.watres.2022.118236

[40] U. Vengatakrishnan, K. Subramanian, V. Rajapand, D.N. Raman, "Effect of Ultraviolet and Solar Radiation on Photocatalytic Dye (Black-E and Congo Red) Degradation Using Copper Oxide Nanostructure Particles," *Iran University of Science and Technology*, vol. 18, no. 3, pp. 1–12, Sep. 2021, http://dx.doi.org/10.22068/ijmse.2145

[41] M.N. Chong, B. Jin, C.W.K. Chow, C. Saint, "Recent developments in photocatalytic water treatment technology: A review," *Water Research*, vol. 44, no. 10, pp. 2997–3027, 2010, https://doi.org/10.1016/j.watres.2010.02.039

[42] S. Ahmed, M.G. Rasul, R. Brown, M.A. Hashib, "Influence of parameters on the heterogeneous photocatalytic degradation of pesticides and phenolic contaminants in wastewater: A short review," *Journal Environmental Management*, vol. 92, no. 3, pp. 311–330, 2011, https://doi.org/10.1016/j.jenvman.2010.08.028

[43] Y. Yu, B.N. Murthy, J.G. Shapter, K.T. Constantopoulos, N.H. Voelcker, A.V. Ellis, "Benzene carboxylic acid derivatized graphene oxide nanosheets on natural zeolites as effective adsorbents for cationic dye removal," *Journal of Hazardous Materials*, vol. 260, pp. 330–338, Sep. 2013, https://doi.org/10.1016/j.jhazmat.2013.05.041

[44] T.D. Kusworo, A.C. Kumoro, M.B. Puspa, P. Citradhitya, D.P. Utomo, "Removal of ciprofloxacin-humic acid pollutant residue in wastewater through a hybrid treatment system consisting of pre-treatment with ozonation-AC/TiO2/CeO2 adsorption and degradation using PVDF/Ni-CeO2@SiO2 photocatalytic membrane," *Journal Environmental Chemical Engineering*, vol. 12, no. 2, Apr. 2024, https://doi.org/10.1016/j.jece.2024.112216

[45] V. Chakachaka, C. Tshangana, O. Mahlangu, B. Mamba, A. Muleja, "Interdependence of Kinetics and Fluid Dynamics in the Design of Photocatalytic Membrane Reactors," *Membranes,* Aug. 01, 2022, MDPI. https://doi.org/10.3390/membranes12080745

[46] I. Fatimah, N.I. Prakoso, I. Sahroni, M.M. Musawwa, Y. Sim, F. Kooli, O. Muraza, "Physicochemical characteristics and photocatalytic performance of TiO2/SiO2 catalyst synthesized using biogenic silica from bamboo leaves," *Heliyon*, vol. 5, no. 11, Nov. 2019, https://doi.org/10.1016/j.heliyon.2019.e02766

[47] E.B. Lied, C.F.M. Morejon, R.L.O. Basso, A.P. Trevisan, P.R.S. Bittencourt, F.L. Fronza, "Photocatalytic degradation of H2S in the gas-phase using a continuous flow reactor coated with TiO2-based acrylic paint," *Environmental Technology*, vol. 40, no. 17, pp. 2276–2289, Jul. 2019, https://doi.org/10.1080/09593330.2018.1440010

[48] N. Ćelić, N. Banic, I. Jagodic, R. Yatskiv, J. Vanis, G. Strbac, S. Lukic-Petrovic, "Eco-Friendly Photoactive Foils Based on ZnO/SnO2-PMMA Nanocomposites with High Reuse Potential," *ACS Applied Polymer Materials*, vol. 5, no. 5, pp. 3792–3800, May 2023, https://doi.org/10.1021/acsapm.3c00396

[49] A.S. Adday, S.M. Al-Jubouri, S. Al-Batty, "Photocatalytic degradation of methylene blue by robust visible-light-driven polyvinylidene fluoride membranes incorporating Ag2O@CRA photocatalyst: Kinetics analysis and cost assessment,'' *Iraqi Journal of Chemical and Petroleum Engineering*, vol. 26, no. 3, pp. 19–28, Sep. 2025, https://doi.org/10.31699/IJCPE.2025.3.3

التحلل الضوئي لصبغة كاتيونية بأستخدام محفز ضوئي نانوي بيضوي الشكل من $Ag_2O@CuO$ تحت الأشعة فوق البنفسجية

دانيه محمد محسن [١،*]، سما محمد الجبوري [١]، سرحان البطي [٢]

١ قسم الهندسة الكيمياوية، كلية الهندسة، جامعة بغداد، بغداد، العراق
٢ قسم تكنولوجيا الهندسة الكيميائية والعمليات، كلية الجبيل الصناعية، مدينة جبيل الصناعية، المملكة العربية السعودية

الخلاصة

تم تحضير المحفز الضوئي $Ag_2O@CuO$ بنجاح بأستخدام طريقة الترسيب المشترك. تم تشخيص المحفز الضوئي المُطوّر باستخدام حيود الأشعة السينية، وتحويل فورييه الطيفي بالأشعة تحت الحمراء، ومطيافية الأشعة السينية، والفحص المجهري للانبعاثات الميدانية، وأطياف الانعكاس المنتشر للأشعة فوق البنفسجية–المرئية، وأطياف التألق الضوئي. تمت دراسة كفاءة $Ag_2O@CuO$ في تحلل رودامين ب (RhB) كصبغة كاتيونية بالتحفيز الضوئي تحت إضاءة الأشعة فوق البنفسجية. ودُرست تأثيرات عوامل مختلفة، مثل نوع الضوء، وجرعة المحفز الضوئي، والتركيز الأولي لRhB، ودرجة حموضة محلول RhB. أظهرت نتائج الدراسة أن تحلل صبغة RhB بنسبة ٩٠% تم الحصول عليه خلال ٩٠ دقيقة عند درجة حموضة ٦,٨ ، و ٥٠ ملغ من جرعة المحفز ، و١٠ ملغ/لتر من صبغة RhB تحت الأشعة فوق البنفسجية. بينما كانت نسبة تحلل الصبغة ٩٨% عند عند درجة حموضة ١٠ وبنفس الظروف الأخرى المذكورة أعلاه. كما تمت دراسة حركية التفاعل بناءً على البيانات التجريبية للتحلل الضوئي التأكسدي لصبغة RhB، حيث تم تطبيق ثلاثة نماذج حركية هي: الموديل الصفري، والموديل من الدرجة الأولى الزائف، ونموذج فريندلخ المعدل. أظهرت النتائج أن الأكسدة الضوئية لصبغة RhB بواسطة المحفز الضوئي غير المتجانس $Ag_2O@CuO$ اتبعت الموديل من الدرجة الأولى الزائف، مع ثابت معدل ظاهري قدره ٠,٠٤٢٩ دقيقة$^{-١}$. علاوةً على ذلك، استُخدم نموذج لانكماير–هينشلوود لنمذجة حركية تحلل RhB الضوئي عند تراكيز ٥ –١٥ ملغم/لتر وتم حساب ثابت معدل التفاعل الضوئي الجوهري وكان ٠,٧١٨٤ ملغم/لتر·دقيقة للمحفز الضوئي غير المتجانس $Ag_2O@CuO$. كما بلغ ثابت الامتزاز المتوازن 0.0767 لتر/ملغم للمحفز الضوئي غير المتجانس $Ag_2O@CuO$.

الكلمات الدالة: أوكسيد الفضة، أوكسيد النحاس، الاكاسيد ثنائية المعدن، الترسيب المشترك، التحفيز الضوئي، صبغة الرودامين ب.